VOL. 10, NO. 4, MARCH 2015 ISSN 1819-6608
ARPN Journal of Engineering and Applied Sciences


www.arpnjournals.com

PERFORMANCE OF ULTRA-WIDEBAND WEARABLE ANTENNA UNDER SEVERE ENVIRONMENTAL CONDITIONS AND SPECIFIC ABSORPTION RATE (SAR) STUDY AT NEAR DISTANCES

Waddah A. M. A. Khairun N. R. and Abdirahman M. S.
Wireless and Radio Science Centre, Universiti Tun Hussein Onn Malaysia, Batu Pahat, Johor, Malaysia
E-Mail: waddahashwal@yahoo.com

ABSTRACT

Two ultra-wideband (UWB) planar monopole antennas have been reported in this paper. The antennas have been developed for wearable application. Worn-systems require flexibility and tolerance against external effects. The substrates of the proposed antennas have been made of jeans while radiators were made of copper tapes. Simulated and measured performances of the antennas in terms of return loss and radiation patterns have been discussed in this work. Recorded results have shown that the operating frequency ranges from 3.04 GHz to 10.3 GHz and from 3.04 GHz to 11.3 GHz with respect to -10 dB for the first and second antennas respectively. The antennas have been tested under severe conditions such as operating in water and aggregates and results have been presented and discussed. Moreover, an extended study on the safety concerns of the antennas by means of specific absorption rate (SAR) has been included in this work. The approximated SAR has been found to be within the safety guidelines set by Federal Communications Commission (FCC).

Keywords: UWB, phantom, SAR, antenna.

1. INTRODUCTION

Ultra-wideband' (UWB) describes that the system/signal possesses a large bandwidth [1]. UWB systems offer high data rate, low cost equipments, multipath immunity and both precise ranging (object location) and high speed communication at the same time. Before UWB technology was commercialized, it has been developed mainly in military radar systems. Today, UWB technology is changing the wireless industry and competing with narrowband technology with its method of spreading signal across a wide range of frequencies instead of broadcasting on separate frequencies [2].

There is the so-called UWB wireless embedded networks (UWEN) project that is working on developing systems with low rate communication for location and tracking applications. Such application targets to improve security of material goods, find our keys, keep pace with children, find people in situations, including fire fighters in burning building, police officers in distress, and track people at recreational activities such as cross country skiing and athletics. The key concept is to develop carried low power UWB devices and data from users transmitted to fixed nodes and exchange signal time of arrival information which enables to determine the location of the device [3].

The increasing growth in using body area networks (BANs), wireless personal area networks (WPANs), and medical sensors has given an interest in wearable antennas that are made for operation on the living bodies. They are found in portable radio equipments used by the military, the pager and mobile phones. The introduction of body worn medical sensors and wireless medical sensor networks has enabled doctors and specialists to monitor patients at a distance [4].

Engineers are not done with only creating remarkable technology such as wearable systems, but also involved in understanding the interaction of electromagnetic (EM) waves with the body in body-centric communications and wireless systems that operate close to the body to understand the nature of electromagnetic properties of body tissues and how they vary significantly with tissue type and frequency. This understanding enables the development of antennas and transceivers for such communications systems. Studying the interaction between EM waves and the body requires modeling of the body with physical phantoms or with numerical phantoms embedded in numerical electromagnetic codes.

With the increase of communication devices that operate close to the human body, the phantoms became an essential tool for testing safety of such devices. Various safety guidelines, such as those by the International Commission on Non-Ionizing Radiation Protection (ICNIRP) [5] and the Institute of Electrical and Electronics Engineers (IEEE) [6], specify the acceptable levels of radiation in terms of specific absorption rate (SAR), which can be measured using a number of methods involving phantoms. Phantoms are also a useful tool in studying of EM wave propagation around and inside the human body. Such studies are necessary to help design powerful, robust, reliable, wearable low-cost communication devices. Phantoms can also provide a steady, controllable propagation environment, which cannot be easily realized with human subjects.

There are many types of broadband directional antennas such as the Vivaldi, log-periodic, cavity-backed, waveguide, horn, and dish antennas that cover the entire 3.1–10.6 GHz band (109%). The undesirable fact about them is that they are electrically large, and have a high profile, while planar monopoles, disc cone, and slot antennas provide omni- and bi-directional radiation patterns and have a low gain and back radiation pattern, therefore they are not suitable for uni-directional

communication [7].

Number of planar UWB antennas has been developed in many ways. In [8], two steps patch with single slot and partial ground plane has been designed. UWB step-slot antenna with a rotated patch was demonstrated in [9]. In [10], a planar microstrip-fed wideband monopole was designed from egg-shaped patch printed off-center depicted a semi-elliptical fractal-complementary slot into the ground plane.

It has been found that the addition of a bevel to the lower corners of the square planar monopole increases the impedance bandwidth as demonstrated in many reported studies. Applying modifications to the bottom edge of the radiating element by using beveling technique has shown that the upper edge frequency is shifted upward [11-16].

In brief, modification techniques are generally used to broaden the impedance bandwidth of small patch antennas and optimize the characteristics of the radiation pattern. These adjustments have an effect on matching mechanism between the radiating element and ground plane. As a result, the bandwidth and the overall size of radiating elements of the antenna are optimized. Planar monopole antennas are good candidates for these techniques and have proven achieving wide impedance bandwidth, omni-directional radiation pattern, compact and simple structure, low cost and ease of construction [7], [17].

The introduction of body-centric networks has led to the development of body worn wireless devices. The body-centric network consists of a number of nodes and units placed on the human body or in close proximity such as on clothing. Body-worn applications require flexible surfaces and circuit components to provide superior electrical and mechanical performances.

This has led to the creation of a new technology using embroidered conductive fibers on polymer. Flexible conductors are constructed from silver-coated p-phenylene-2, 6-benzobisoxazole (PBO) fibers (e-fibers). The e-fibers provides inherent mechanical strength (due to their polymer core), together with high electrical conductivity owed to the silver coating. Lightweight and conformal electro-textiles based on conductive threads and fabrics provide compelling means to fabricate seamlessly garment-integrated antennas substrates [18], [19].

Wearable tags are meant to be used near the body. As a result, the human body absorbs RF energy, reducing the overall antenna performance. In this application, also humidity, bending, and stretching likely affect the performance of the antenna. Sewing pattern and thread densities can also affect the overall performance of an embroidered antenna as investigated in [20].

In [21], authors have investigated the feasibility of the ultra-wideband half-disk structures based on camouflage cloth (substrate) compared to the performance of solid copper and woven versions (radiators). The study has concluded that solid copper version has shown good measured return loss characteristics, omni-directional patterns, and acceptable transient response.

In [22], the authors proposes three different antenna structures. The substrate of the designed antennas was made from two types of fabrics: jeans and flannel. The dimensions of the proposed antennas are 40 mm × 40 mm for antenna I, and 60 mm × 60 mm for antenna II and III.

SAR is the time derivative (rate) of the incremental energy (dW) absorbed by (dissipated in) an incremental mass (dm) contained in a volume element (dV) of a given density (ρ).

$$SAR = \frac{d}{dt}\left(\frac{dW}{dm}\right) = \frac{d}{dt}\left(\frac{dW}{\rho dV}\right) \quad (1)$$

SAR is expressed in units of watts per kilogram (W/kg) or equivalently milliwatts per gram (mW/g). Some refer to it as a so-called volume-SAR, expressed in units of mW/cm^3, where mass density has been set to unity. SAR can be related to the E-field at a point as in equation (2)

$$SAR = \frac{\sigma |E|^2}{\rho} \quad (2)$$

Where σ is conductivity of the tissue (S/m), ρ is mass density of the tissue (kg/m^3) and E is the electric field strength (V/m).

Specific absorption rate—peak spatial-average is determined by the maximum local SAR averaged over a specified volume or mass, e.g., any 1 g or 10 g of tissue in the shape of a cube. SAR is expressed in W/kg or equivalently mW/g.

Most of the studies of wearable antennas have not stepped into the area of Specific Absorption Rates (SAR) test, which is required to study the power absorption issues and meet the standards in order to avoid harm to human body. The aim of this study includes producing antennas with smaller geometries and low SAR.

A considerable attention has been given to the impact of the interaction between electromagnetic (EM) fields and the human body as in [23]–[26]. The interaction between human head and cellular phones has been studied in [27], [28], while interaction between human head and terminal antennas has been studied in [29], [30]. These works have been conducted in order to examine whether or not the antenna radiation exceed the limits set by the standards [5], [31].

Studies on the evaluation of the power absorbed by human body and the Specific Absorption Rate (SAR) have been conducted in different methods. Kuster [27] has evaluated the absorption mechanism for homogenous body model while Kivekas [32] has considered homogenous and layered body model. Klemm [33] has further studied the interactions of UWB antennas used in wearable applications on homogenous and layered human body models. SAR results of very near antennas to the body have been computed in order to investigate the influence of the body. The first evaluation of SAR was on a simple homogenous model composing one tissue

(muscle of 50 mm thickness). The second model consisted of three-layers (skin: 0.5, 1 and 2 mm; fat: 1, 3 and 6 mm; muscle: 50 mm). The study assumed all models to be planar neglecting the curvature of the body.

In [34], a simple evaluation method of estimating local average SAR has been proposed based on COST244 cubical and spherical head model (numerical phantom), followed by studying the effect of the distance and the frequency on the average SAR and comparing the obtained evaluations with realistic head model. Lightweight spherical COST244 tissue-equivalent phantom for evaluation of antenna performances has been proposed in [35].

Gabriel [36], has proposed phantom hand materials based on carbon-loaded silicones and demonstrated within the frequency range 600–6000 MHz. A broadband skin-equivalent semi-solid phantom was introduced in [37] for measuring values of the human skin permittivity in the 55–65 GHz range. In [38], a tissue-mimicking phantom materials has been proposed. Authors have characterized oil-in-gelatin dispersions to approximate value of the dispersive dielectric properties of a variety of human soft tissues within the range of 500 MHz - 20 GHz. Different tissues are mimicked by selection of an appropriate concentration of the proposed material.

A summarized study on electromagnetic properties and modeling of the human body has been reported in [39]. The flowchart shown in Figure-1 illustrates the aspects that have been followed for the proposed work.

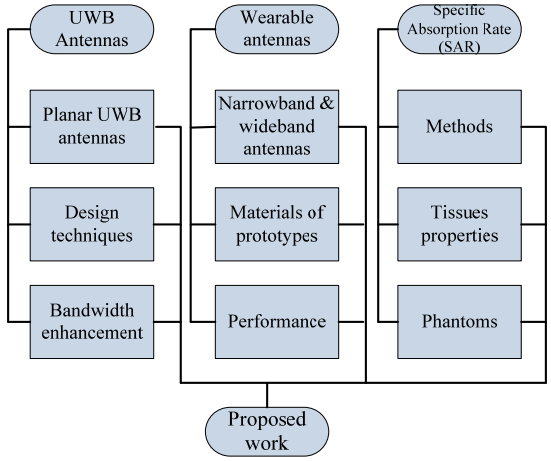

Figure-1. Methodology of the research.

2. EXPERIMENTAL MODELS

Two planar monopole antennas operating within the range of UWB have been developed and presented in this paper. The following summarizes an extensive study on the performances of the proposed designs and concluded with an approximation for the specific absorption rate (SAR) of the antennas under study.

Antenna materials

The proposed antennas have been developed from jeans as a substrate and copper tapes as radiators to provide flexibility for the wearer.

The properties of the jeans used for building the substrate of the antennas have been obtained and measured at early stage. Results have been reported in previous work [40]. The experimental results suggest that the permittivity and loss tangent are 1.76 and 0,078 respectively.

Antenna design

The proposed antennas have overall sizes of 46 × 46 mm^2 and 32 × 34 mm^2 with thickness of 1 mm.

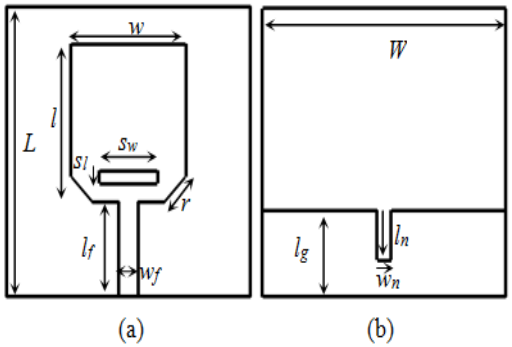

Figure-2. First proposed antenna, size 46 × 46 mm^2 ,a) front and b) back view [40].

Detailed dimensions of the antenna have been reported in [40] and [41]. In previous published work, few aspects have been covered such as simulated and measured return loss results for the antennas at free space, simulated radiation patterns and SAR evaluation when antennas are placed at a fixed point. This paper includes an extended experimental work for the performance of the antennas when applying an external force such as bending and examining the tolerance of the antennas at severe conditions such as soaking in water and burying in aggregates. Measurement of radiation patterns is also reported in this paper.

3. RESULTS AND DISCUSSIONS

The proposed designs have been tested under severe conditions to examine their robustness and ability to sustain an acceptable operating frequency. The top corners of the antennas have been bent towards each other as shown in Figure-3(a) and 3(b). Figure-3(c) shows how the antennas were bent from one of the corners at the top towards a corner located at the end of its diagonal, while Figure-3(d) shows how the antennas were rolled from their top part towards the bottom part. Figure-4(a), (b) and (c) illustrate the measured results of the return loss when different bending situations are applied to the first proposed antenna. It can be seen that the antenna sustains its return loss to a good shape. The antenna has been then tested when placed very close to an arm and results are shown in Figure-4(d). The proposed antenna has shown

that it can withstand severe conditions with succeeding to keep its operating bandwidth as desirable.

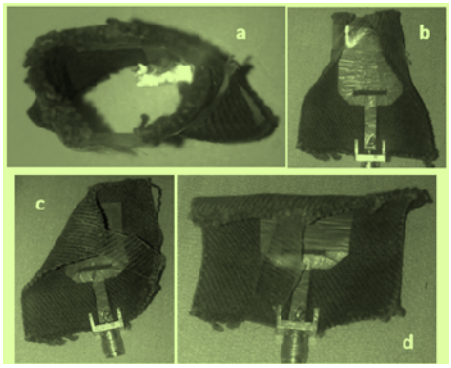

Figure-3. Antennas under bending test.

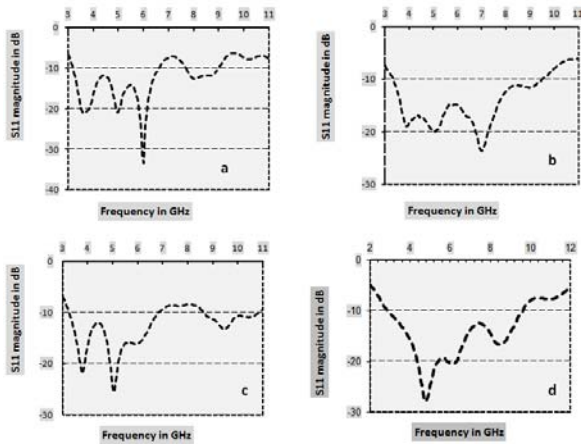

Figure-4. Measured results for the first proposed antenna at bend conditions.

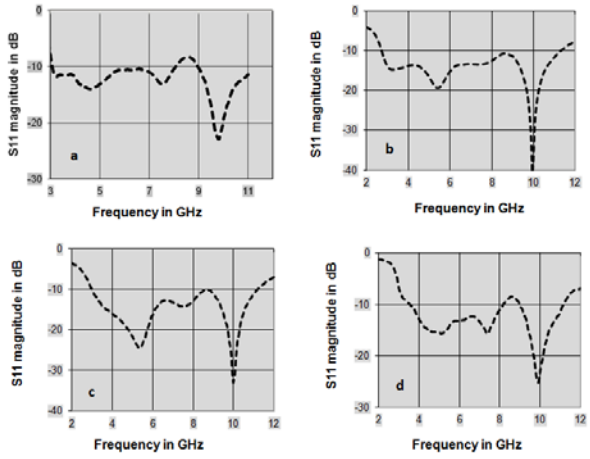

Figure-5. Measured results for the second proposed antenna at bend conditions.

As the aim of the project to produce flexible wearable antennas, both of the antennas have been tested under very severe environmental conditions. Expecting the user is a person whose uniform may endure wetness, sands or mud, the following experiments have included testing the performance of the antennas (namely antenna I and antenna II) at conditions such as: soaking the antennas in water, burying in fine aggregates and finally testing the antennas when both of the conditions are present. Figure-6 shows pictures of these experiments. The measurement of the return loss has been taken for the frequency range from 2 GHz to 11 GHz at room temperature. In order to prevent the network analyzer from any damage, the antennas have been soaked to a level beneath SMA connector to prevent water from leaking into the cable.

Figure-6. Testing setup for the proposed designs.

The results of the experiment are illustrated as a comparison between the two proposed designs.

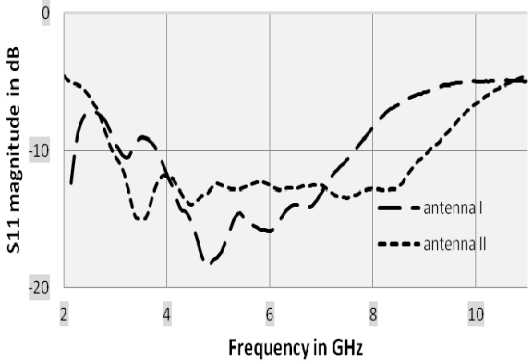

Figure-7. Antennas buried in fine aggregates.

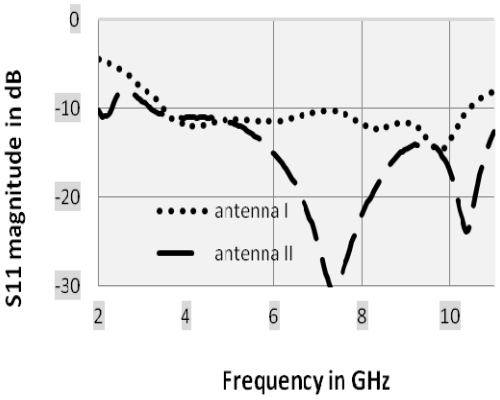

Figure-8. Antennas in water with a plastic bag.

The results in Figure-7 show that the antennas have a good chance to keep operating within an acceptable

bandwidth. It can be seen that antenna II (the second proposed design) performance is much better than antenna I; as it has a wider operating frequency.

The results shown in Figure-8 represent the performance of the antennas when soaked in water while casing with a plastic bag. Figure-9 shows the performance when removing the plastic bag. It is observed that the antennas have a better return loss level when preventing water from wetting the substrate especially the region between the feed-line and the ground-plane; that is the direct contact with water causes a short circuit, which disturbs the inductance and capacitance of the impedance, which results in a poor matching and return loss.

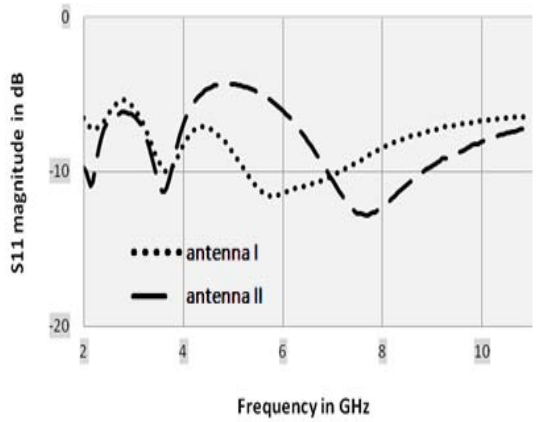

Figure-9. Antennas in water without a plastic bag.

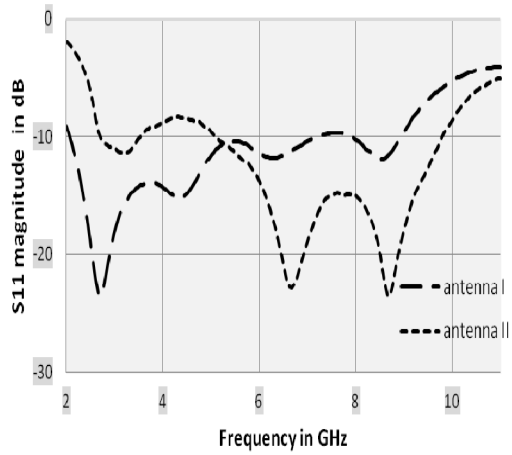

Figure-10. Return loss for the antennas 10 minutes after exposure to the sun.

Figure-10 illustrates the performance of the antennas after being exposed to the sun heat for 10 minutes approximately after they were soaked in water in early stage. It can be observed that both of the antennas have a good operating frequency throughout a wide range. It is also observed that antenna I has a better performance at the lower band, while antenna II at the upper range frequencies.

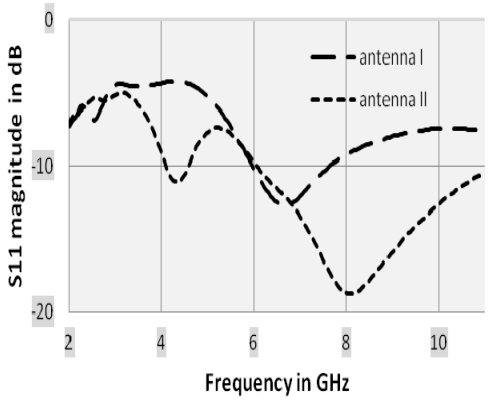

Figure-11. Return loss for the antennas inside (aggregates + water).

The performance of the antennas has been recorded after burying the antennas in fine aggregates after adding water. It is observed from Figure-11 that the return loss of both of the antennas has deteriorated significantly, except that antenna II has an acceptable return loss at higher frequencies.

In conclusion, it can be noticed from the experiments conducted to test the stability of the proposed designs that the antennas have a good record of performance at severe environmental conditions. It is also observed that the second proposed design, antenna II, has a better record than antenna I. It is possible to relate that to the complexity of the geometry of the design, where the design of antenna II has been simplified to a rectangular patch and partial ground without adding any other small patterns to the design such as slots and notches that are used to reroute the path of current flow on the radiator to enhance or change the impedance bandwidth. Changes to these patterns such as expanding or shrinking can significantly affect the flow of the current and have an impact to the overall performance of the antenna.

Lastly, radiation pattern measurements have been taken for both proposed antennas. Figure-12 and Figure-13 show the plotted patterns of E-field at vertical and horizontal orientation for the first and second proposed antennas respectively (antenna I and antenna II). The measurements are shown for frequencies 3 GHz, 4 GHz, 5 GHz and 6 GHz. It can be seen that the antenna has circle-like patterns at vertical orientation. The patterns have taken different shape when measured at horizontal orientation. It is observed that the antenna has donut-like at frequencies 5 GHz and 6 GHz. It can be seen that the E-field strength decreases as the frequency increases as shown for 3 GHz where E-field has a value of nearly 125 dBμV/m, while it drops to lower than 100 dBμV/m for both of vertical and horizontal orientation.

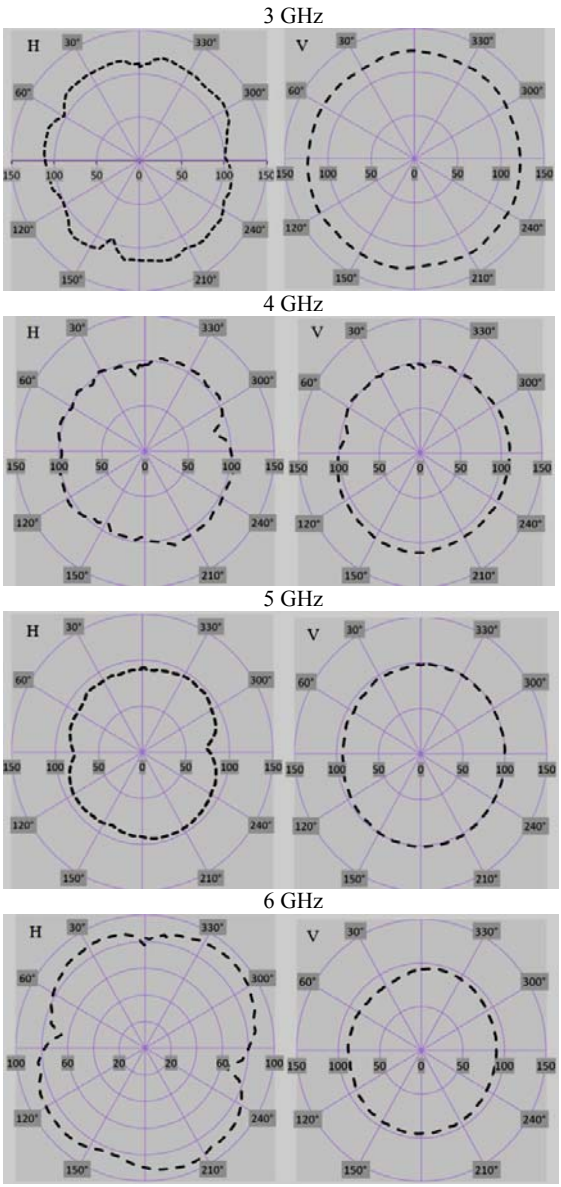

Figure-12. Radiation pattern of antenna I (units: dBµV/m).

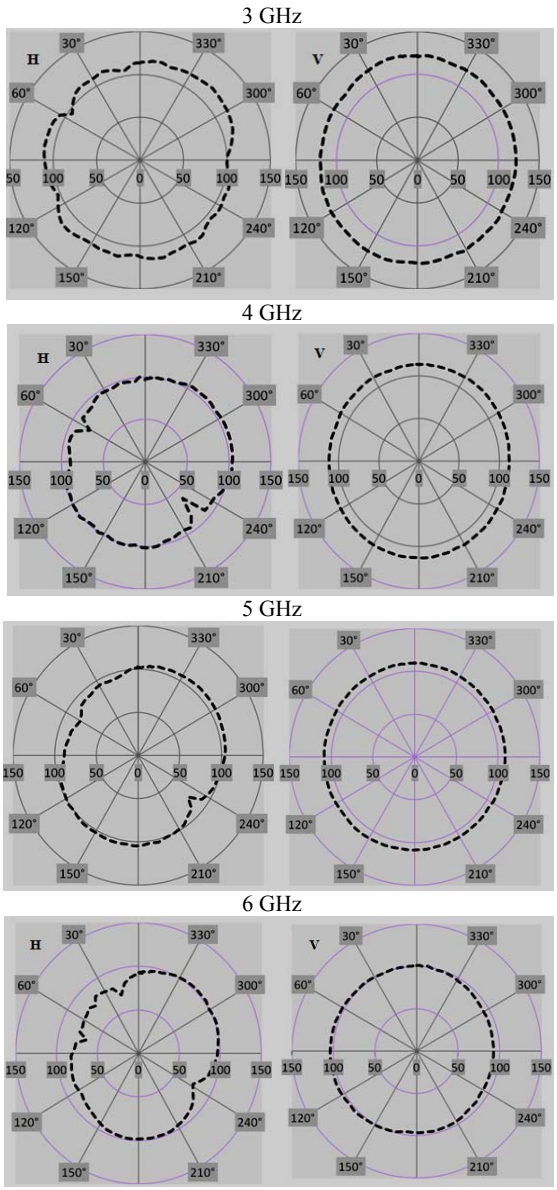

Figure-13. Radiation pattern of antenna II (units: dBµV/m).

4. PHANTOM MODEL FOR SPECIFIC ABSORPTION RATE (SAR)

The methodology of developing this model is based on [27], [32] and [33]. CST STUDIO SUITE developers have also shared a note on "BODY WEARABLE ANTENNA Simulation Challenges" of RFID, ISM and UWB antennas [42]. The note discusses construction and body model handling when dealing with complex geometries. The minimum specifications of hardware suggested for proper performance is also included (for homogenous model at $\varepsilon_r = 42$). Figure-14 shows a worn antenna on a homogenous phantom and corresponding mesh cells, memory, time, and hardware amounts for full body size. These figures are based on Intel® Xeon® E5620 2.4 GHz CPU, 4×Tesla 2070 GPUs.

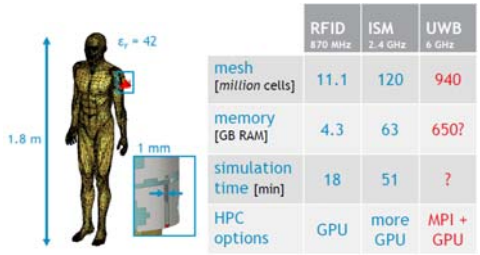

Figure-14. Model size and required.

Homogenous phantom is a one layer model with one dielectric constant, while voxel phantom is more complex and has an excellent mimic with the human body. Dielectric properties vary with the distribution of the human body layers as we go deeper. Figure-15 shows homogenous and voxel phantoms.

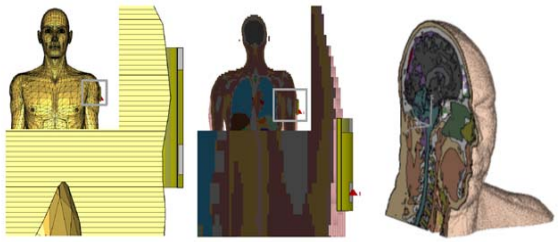

(a) (b) (c)

Figure-15. (a) homogenous phantom, (b) voxel phantom, (c) cross-section of voxel phantom.

The note has also included a comparison between homogenous and voxel phantoms in terms of S11 and SAR considering full and partial body. The difference was found to be in small fractions (according to the example studied in the note: SAR: 0.667 W/kg for homogenous model and SAR: 0.883 W/kg for voxel model). It also studied the same example on full and reduced model. The result was found to be very close (SAR: 0.667 W/kg for full homogeneous body model and SAR: 0.644 W/kg for partial homogeneous body model). Based on the available information, our developed model can provide a closer approximation for the performance of the antenna than the homogenous model does. Since the model consists of multiple layers with different permittivity, which makes it closer to voxel model to a certain level. This model is found to be cheaper and less complex when carrying out simulation tests for wearable antennas on personal computer with lower specifications.

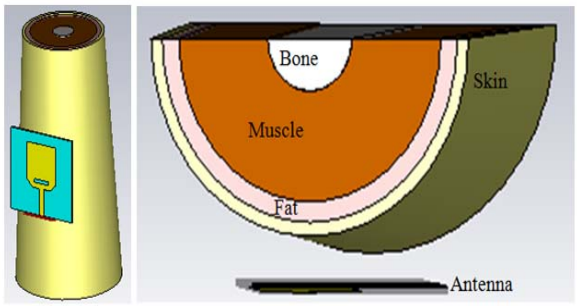

(a) (b)

Figure-16. Human arm model developed in CST MWS, a) perspective view, b) cross section of the top view (zoomed in).

As mentioned previously, the performance of proposed antennas operating in close proximity to the body has been conducted using developed numerical human arm model (phantom). The model was developed in CST Microwave Studio. It simply represents a portion of the human body; that is the arm. Four-layer model (skin, fat, muscle and bone) has been considered for the evaluation. Curvature of the body part has been approximated to a conical shape with top and bottom radiuses. The thickness of each layer was taken as: skin = 2 mm, fat = 3 mm, muscle = 8 mm and bone = 10 mm (radius) as in [33] and [43]. Figure-16 illustrates the arm model developed in CST MWS and the orientation of the antenna with respect to the model. The model consists of bone (centre), muscle, fat, and skin (outer layer).

The total 10-g SAR for the two proposed antennas has been evaluated for selected frequencies at different distances. The graphic illustration in Figure-18 and Figure-19 show the total SAR for frequencies 3 GHz, 5 GHz, 7 GHz and 9 GHz at 5 mm, 10 mm, 15 mm and 20 mm placements from the phantom.

The computed values plotted in Figure-17 show that the antenna has very low total SAR as the antenna is placed farther from the phantom. This can be seen more clearly at the lower band frequencies such as 3 GHz and 5 GHz, where the total SAR for 3 GHz has reduced from more than 6 W/kg at 5 mm to lower than 3 W/kg at 20 mm. It can be understood that the phantom has a bigger chance to absorb more radiated and reflected power at near spacing than far one.

The graph also shows how the total SAR decreases as the frequency increases for a fixed distance, where the total SAR at 5 mm reduces from more than 6 W/kg at 3 GHz to about 1 W/kg at 9 GHz.

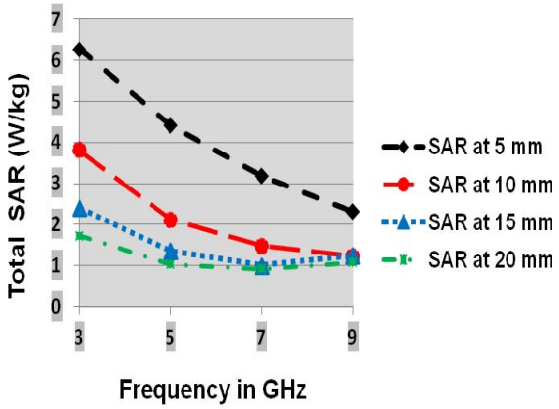

Figure-17. Total SAR [W/kg] for antenna I in the 4-layer body phantom.

The SAR results for 10-g change with the frequency. This could be regarded to the fact that human tissues are anisotropic mediums. The difference in the internal structure of the model has caused different responses for the penetrating radiations. The conductivity of the skin is the main player in the absorption of the radiated power. The skin has the highest conductivity followed by muscle and bone layers, while the fat has the lowest. This explains that most of the absorbed power occurs on the skin.

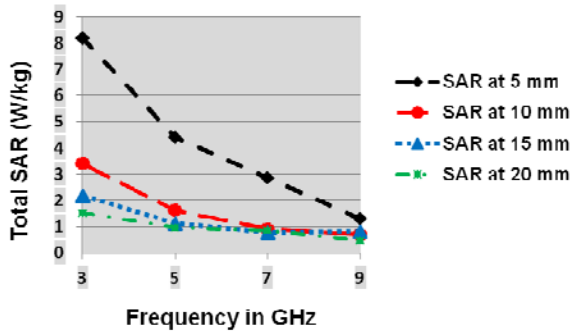

Figure-18. Total SAR [W/kg] for antenna II in the 4-layer body phantom.

The plotted values in Figure-18 represent the total SAR for antenna II. It can be observed how the SAR of the antenna reduces as the antenna is placed farther from the phantom. The value of SAR from 3 GHz at 5 mm is observed to be higher than the one for antenna I. The drop of SAR values in Figure-18 has a smother look than the one in Figure-18. Here, it is worthwhile to recall the nature of the design of both of the antennas, where antenna I has been designed with symmetrical geometry unlike antenna II which was designed asymmetrical. Therefore, the same portion of the phantom could have absorbed more power from antenna II than antenna I at that particular frequency, and this significantly depends on the patterns of the electric-field.

5. CONCLUSIONS

The study of on-body systems has widened the research about the quality of the performance of the wearable antennas when attached to the body and the impact of the interaction between the radio-waves and tissues of the body. To provide such information about the interaction between the electromagnetic radiations and the living body, researchers and mobile industries have developed a representation for the human body to examine the behavior of both of the communicating device and the so-called phantom. These phantoms or representations come in either physical or numerical objects.

Physical phantoms are made of materials that have approximately similar properties, such as permittivity, to the human tissues. Numerical phantoms have proved that they provide agreeable readings as the physical phantoms do. Specific absorption rate (SAR) is one of the important information that can be obtained. SAR provides an idea on how the antenna affects the tissue and the degree of safety.

This report has summarized some previous efforts on the evaluation of the effects of EMF on the human body caused by communication systems. Some studies have evaluated the power absorbed by the human body and the specific absorption rate by using homogenous and inhomogeneous phantom models. The proposed model consists of four-layer body tissues with approximated curvature to arm shape. The antenna performance at the presence of the body has been obtained and discussed. The SAR evaluation has been performed. The proposed antennas meet the permissible limit of radiation and are safe to use.

The proposed antennas have been made on jeans substrate whose dielectric constant had been measured. The design of each of the two proposed antennas has followed different approaches. The first proposed antenna was designed using different techniques such as bevels, slots and notches in order to achieve a high bandwidth. The second proposed antenna was designed in simpler approach using a mere rectangular patch on a partial ground-plane without adding any techniques in order to ease producing the antenna and minimize the errors at fabrication stage.

Simulated and measured S11 parameter results of the antennas at free space have shown an improved bandwidth that covers the entire range of UWB. Performance of the antennas operating in close proximity to the phantom has been included in this work. Since the developed antennas were proposed for wearable applications, number of experiment has been conducted to examine the stability of the antenna at selected conditions. Conditions such as bending the antennas to a certain degree were applied and results have been discussed. Further investigations have been added to the work to examine the operation of the antennas when severe environmental conditions such as soaking the antennas in water or buried in fine aggregates. The proposed antennas have passed the minimum requirements for UWB which is 25% of bandwidth.

ACKNOWLEDGEMENTS

The authors would like to thank UTHM for sponsoring this work under the reference UTHM/PPI/600-5/1/10 Jilid 7(45). The authors would like also to appreciate the Ministry of Higher Education, Yemen for their contribution into the research.

6. REFERENCES

[1] B. Allen., M. Dohler., E. Okon., W. Q. Malik., A. K. Brown. and D. J. Edwards. Ultra-wideband: antennas and propagation for communications, radar and imaging. Chichester, UK: John Wiley & Sons, Ltd, 2006.

[2] M. Ghavami., L. Michael. and R. Kohno. Ultra Wideband Signals and Systems in Communication Engineering. Wiley, 2004.

[3] K. Siwiak. and D. McKeown. Ultra-Wideband Radio Technology. Chichester, UK: John Wiley & Sons, Ltd, 2004.

[4] D. Guha. and Y. M. M. Antar. Microstrip and Printed Antennas. Chichester, UK: John Wiley & Sons, Ltd, 2010.

[5] A. Ahlbom., U. Bergqvist., J. H. Bernhardt., J. P. Cesarini., M. Grandolfo., M. Hietanen., A. F. Mckinlay., M. H. Repacholi., D. H. Sliney., J. A. J. Stolwijk. and others. "Guidelines for limiting exposure to time-varying electric, magnetic, and electromagnetic fields (up to 300 GHz). International Commission on Non-Ionizing Radiation Protection.," Heal. Phys, vol. 74, no. 4, pp. 494–522, 1998.

[6] "IEEE Recommended Practice for Determining the Peak Spatial-Average Specific Absorption Rate (SAR) in the Human Head from Wireless Communications Devices: Measurement Techniques," IEEE Std 1528-2003, pp. 1–120, 2003.

[7] R. Azim., M. T. Islam. and N. Misran. "Printed Planar Antenna for Wideband Applications," J. Infrared, Millimeter, Terahertz Waves, pp. 969–978, May 2010.

[8] S. H. Choi., J. K. Park., S. K. Kim. and J. Y. Park. "A new ultra-wideband antenna for UWB applications," Microw. Opt. Technol. Lett., vol. 40, no. 5, pp. 399–401, March. 2004.

[9] K. Song., Y. Yin., B. Chen., S. Fan. and F. Gao. "Bandwidth Enhancement Design of Compact UWB Step-Slot Antenna with Rotated Patch," in Progress In Electromagnetics. 2011. vol. 22, no. March, pp. 39–45.

[10] C. Sim. "A Compact Monopole Antenna for Super Wideband Applications," IEEE Antennas Wirel. Propag. Lett., vol. 10, pp. 488–491, 2011.

.[11]A. Antonino-Daviu., E. and Cabedo-Fabres. M. Ferrando-Bataller. M. and Valero-Nogueira. "Wideband double-fed planar monopole antennas," Electron. Lett., vol. 39, no. 23, pp. 3–4, 2003.

[12] Z. N. Chen., T. S. P. See. and X. Qing. "Small Printed Ultrawideband Antenna With Reduced Ground Plane Effect," IEEE Trans. Antennas Propag., vol. 55, no. 2, pp. 383–388, February. 2007.

[13] C.-Y. Hong., C.-W. Ling., I.-Y. Tarn. and S.-J. Chung. "Design of a Planar Ultrawideband Antenna With a New Band-Notch Structure," IEEE Trans. Antennas Propag., vol. 55, no. 12, pp. 3391–3397, December. 2007.

[14] K. Koski., A. Vena., L. Sydanheimo., L. Ukkonen. and Y. Rahmat-Samii. "Design and Implementation of Electro-Textile Ground Planes for Wearable UHF RFID Patch Tag Antennas," IEEE Antennas Wirel. Propag. Lett., vol. 12, pp. 964–967, 2013.

[15] P. Thomas., D. D. Krishna., M. Gopikrishna., U. G. Kalappura. and C. K. Aanandan. "Compact planar ultra-wideband bevelled monopole for portable UWB systems," Electron. Lett., vol. 47, no. 20, p. 1112, 2011.

[16] K. Zhang., Y. Li. and Y. Long. "Band-Notched UWB Printed Monopole Antenna With a Novel Segmented Circular Patch," IEEE Antennas Wirel. Propag. Lett., vol. 9, pp. 1209–1212, 2010.

[17] M. GOUDA. and M. Y. M. YOUSEF. "Bandwidth Enhancement Techniques Comparison for Ultra Wideband Microstrip Antennas for Wireless Application," J. Theor. Appl. Inf. Technol., vol. 35, no. 2, pp. 184–193, 2012.

[18] L. Zhang., Z. Wang. and J. L. Volakis. "Textile Antennas and Sensors for Body-Worn Applications," IEEE Antennas Wirel. Propag. Lett., vol. 11, pp. 1690–1693, 2012.

[19] K. Koski., A. Vena. and L. Sydanheimo. "Design and implementation of electro-textile ground planes for wearable UHF RFID patch tag antennas," vol. 12, pp. 1590–1593, 2013.

[20] E. Moradi., T. Bjorninen., L. Ukkonen. and Y. Rahmat-Samii. "Effects of Sewing Pattern on the Performance of Embroidered Dipole-Type RFID Tag Antennas," IEEE Antennas Wirel. Propag. Lett., vol. 11, pp. 1482–1485, 2012.

[21] W. Davis. and W. Stutzman. "Wearable Ultra-Wideband Half-Disk Antennas," in 2005 IEEE Antennas and Propagation Society International Symposium, 2005, vol. 3A, pp. 500–503.

[22] M. A. R. Osman., M. K. A. Rahim., N. A. Samsuri. and M. E. Ali. "Compact and embroidered textile wearable antenna," in 2011 IEEE International RF & Microwave Conference, 2011, vol. 4, no. December, pp. 311–314.

[23] M. A. Stuchly. "Electromagnetic fields and health," IEEE Potentials, vol. 12, no. 2, pp. 34–39, Apr. 1993.

[24] A. Rosen., M. A. Stuchly. and A. Vander Vorst. "Applications of RF/microwaves in medicine," IEEE Trans. Microw. Theory Tech., vol. 50, no. 3, pp. 963–974, March. 2002.

[25] I. Chatterjee., M. J. Hagmann. and O. P. Gandhi. "Electromagnetic absorption in a multilayered slab model of tissue under near-field exposure conditions," Bioelectromagnetics, vol. 1, no. 4, pp. 379–388, 1980.

[26] I. Chatterjee., O. P. Gandhi., M. J. Hagmann. and A. Riazi. "Plane-wave spectrum approach for the calculation of electromagnetic absorption under near-

field exposure conditions," Bioelectromagnetics, vol. 1, no. 4, pp. 363–377, 1980.

[27] N. Kuster. and Q. Balzano. "Energy absorption mechanism by biological bodies in the near field of dipole antennas above 300 MHz," IEEE Trans. Veh. Technol., vol. 41, no. 1, pp. 17–23, 1992.

[28] K. Meier., V. Hombach., R. Kastle., and N. Kuster. "The dependence of electromagnetic energy absorption upon human-head modeling at 1800 MHz," IEEE Trans. Microw. Theory Tech., vol. 45, no. 11, pp. 2058–2062, 1997.

[29] O. P. Gandhi., G. Lazzi. and C. M. Furse. "Electromagnetic absorption in the human head and neck for mobile telephones at 835 and 1900 MHz," IEEE Trans. Microw. Theory Tech., vol. 44, no. 10, pp. 1884–1897, 1996.

[30] A. Christ. and N. Kuster. "Differences in RF energy absorption in the heads of adults and children," Bioelectromagnetics, vol. 26, no. S7, pp. S31–S44, 2005.

[31] A. ANSI. "IEEE C95. 1-1992: IEEE Standard for Safety Levels with Respect to Human Exposure to Radio Frequency Electromagnetic Fields, 3 kHz to 300 GHz, The," Inc., New York, NY, 1992.

[32] O. Kivekäs., T. Lehtiniemi. and P. Vainikainen. "On the general energy-absorption mechanism in the human tissue," Microw. Opt. Technol. Lett., vol. 43, no. 3, pp. 195–201, Nov. 2004.

[33] M. Klemm. and G. Troester. "EM Energy Absorption In The Human Body Tissues Due To Uwb Antennas," Prog. Electromagn. Res., vol. 62, pp. 261–280, 2006.

[34] H. Kawai. and K. Ito. "Simple Evaluation Method of Estimating Local Average SAR," IEEE Trans. Microw. Theory Tech., vol. 52, no. 8, pp. 2021–2029, August. 2004.

[35] H. Yamaguchi., H. Arai., Y. Shimizu. and T. Tanaka. "Lightweight tissue-equivalent phantom for evaluation of antenna performances," 2008 Asia-Pacific Microw. Conf., pp. 1–4, December. 2008.

[36] C. Gabriel. "Tissue equivalent material for hand phantoms.," Phys. Med. Biol., vol. 52, no. 14, pp. 4205–10, July. 2007.

[37] N. Chahat., M. Zhadobov. and R. Sauleau. "Broadband Tissue-Equivalent Phantom for BAN Applications at Millimeter Waves," IEEE Trans. Microw. Theory Tech., vol. 60, no. 7, pp. 2259–2266, July. 2012.

[38] M. Lazebnik., E. L. Madsen., G. R. Frank. and S. C. Hagness. "Tissue-mimicking phantom materials for narrowband and ultrawideband microwave applications.," Phys. Med. Biol., vol. 50, no. 18, pp. 4245–58, September. 2005.

[39] Y. Hao. and A. Alomainy. "Antennas and Propagation for Body-Centric Wireless Communications," IEEE Antennas Propag. Mag., vol. 50, no. 2, pp. 148–148, Apr. 2008.

[40] W. A. M. Al Ashwal. and K. N. Ramli. "Compact UWB wearable antenna with improved bandwidth and low SAR," in 2013 IEEE International RF and Microwave Conference (RFM), 2013, pp. 90–94.

[41] W. A. M. Al Ashwal. and K. N. Ramli. "Compact UWB wearable antenna with improved bandwidth and low SAR," in 2013 IEEE International RF and Microwave Conference (RFM), 2013, pp. 90–94.

[42] M. Rütschlin. "BODY WEARABLE ANTENNA simulation challenges," in Euroupean User Conference, 2013.

[43] M. L. Scarpello., D. Kurup., H. Rogier., D. Vande Ginste., F. Axisa., J. Vanfleteren., W. Joseph., L. Martens. and G. Vermeeren. "Design of an Implantable Slot Dipole Conformal Flexible Antenna for Biomedical Applications," IEEE Trans. Antennas Propag., vol. 59, no. 10, pp. 3556–3564, October, 2011.